

# A Model to Study the Effect of $\text{Na}^+$ ions on $\text{Ca}^{2+}$ diffusion under Rapid Buffering Approximation

Vikas Tewari and K.R. Pardasani

**Abstract**—Calcium is very important for communication among the neurons. It is vital in a number of cell processes such as secretion, cell movement, cell differentiation. To reduce the system of reaction-diffusion equations of  $[\text{Ca}^{2+}]$  into a single equation, two theories have been proposed one is excess buffer approximation (EBA) other is rapid buffer approximation (RBA). The RBA is more realistic than the EBA as it considers both the mobile and stationary endogenous buffers. It is valid near the mouth of the channel. In this work we have studied the effects of different types of buffers on calcium diffusion under RBA. The novel thing studied is the effect of sodium ions on calcium diffusion. The model has been made realistic by considering factors such as variable  $[\text{Ca}^{2+}]$ ,  $[\text{Na}^+]$  sources, sodium-calcium exchange protein (NCX), Sarcolemmal Calcium ATPase pump. The proposed mathematical leads to a system of partial differential equations which has been solved numerically to study the relationships between different parameters such as buffer concentration, buffer disassociation rate, calcium permeability. We have used Forward Time Centred Space (FTCS) approach to solve the system of partial differential equations.

**Keywords**—rapid buffer approximation, sodium-calcium exchange protein, Sarcolemmal Calcium ATPase pump, buffer disassociation rate, forward time centred space.

## I. INTRODUCTION

**C**ALCIUM  $[\text{Ca}^{2+}]$  plays an important role in a number of processes like cell movement, muscle contraction, gene expression, synaptic plasticity, etc.

It helps in the mechanism of exocytosis by combining with synaptotagmin to release neurotransmitters. It is used in signal transduction where an electrical signal is converted into chemical signal. Local  $[\text{Ca}^{2+}]$  elevations participate in the calcium signaling by regulating calcium-gated plasma membrane ion channels [9].  $[\text{Ca}^{2+}]$  enters a cell via ion channels and redistributes itself throughout the cell via diffusion. Experiments have shown that a number of parameters like buffer concentration, Sarcolemmal Calcium ATPase pump,  $\text{Na}^+$ - $\text{Ca}^{2+}$  exchange (NCX) protein, Endoplasmic Reticulum (ER) stores,  $\text{Na}^+$ - $\text{K}^+$  ATPase pump affect the behaviour of  $[\text{Ca}^{2+}]$ . So in order to have a complete model for cytosolic  $[\text{Ca}^{2+}]$  behaviour we should incorporate all the possible necessary parameters.  $[\text{Ca}^{2+}]$  is strongly buffered in living cells. A number of experiments conducted in various cell types suggest that only 1 – 5% of calcium ions in the cytoplasm are free, i.e., not bound to buffers [9] [12]. RBA is valid near the mouth of calcium channel [12]. The high affinity buffers affect

calcium signaling mechanisms, granule exocytosis, excitation contraction coupling and a variety of other mechanisms in which changes in calcium concentrations are important [10]. Cellular calcium buffers, whether stationary or mobile, reduce the free calcium concentration and localize calcium signals by reducing the effective diffusion coefficient for calcium [1]. RBA assumes that the buffering time scales are rapid, reaching equilibrium at each point in space before appreciable diffusion occurs, [12]. Both i.e., EBA and RBA assume hemispherical symmetry and a point source for calcium ions. These two approximations are complimentary in the sense that they are valid in different parameter regimes, but it is important to note that in some cases neither approximation can be applied, [9].

Another factor which might have significant effect on  $[\text{Ca}^{2+}]$  diffusion and which has not been given much importance till date is the sodium ion concentration. Calcium extrusion in heart muscles is caused by the electrochemical sodium gradient across the plasma membrane. The dependence of  $\text{Na}^+$  –  $\text{Ca}^{2+}$  electrochemical gradient has been studied by Sheu and Fozzard for sheep ventricular muscle and Purkinje strands. It has been observed that the sodium gradient across the plasma membrane influences the intracellular calcium concentration via a counter-transport of sodium for calcium ion. Fujioka et al. [4] also found that NCX is the major mechanism by which cytoplasmic calcium is extruded from cardiac myocytes. Thus, there is enough evidence that  $\text{Na}^+$  is an important parameter to be considered when modelling cytosolic  $[\text{Ca}^{2+}]$  concentration. Thus, in our model, we have considered NCX with an exchange ratio of 4:1 [4] with respect to sodium and calcium ion respectively, to study the effect of sodium influx over cytoplasmic calcium profile. Other novel features incorporated in the model are a variable calcium and sodium source instead of a constant source to study the effects of calcium and sodium permeabilities on calcium and sodium ions respectively. The proposed model has a Sarcolemmal Calcium ATPase pump (SL  $\text{Ca}^{2+}$  ATPase pump) which is expressed in Hill's equation form with a Hill's coefficient of 1.6 [8]. For simulation of the model we have used Finite Difference Method (Forward Time Centered Space) approach. A MATLAB program has been developed for the above process and simulated on a Pentium IV Dual Core, 1.00 GB RAM, 1.73GHz processor to obtain the numerical result. The time taken per simulation is 240 seconds for time,  $t = 10$  milliseconds.

## II. MATHEMATICAL MODEL

Our mathematical model assumes the following reaction-diffusion kinetics [9] [12],

Vikas Tewari is with the Maulana Azad National Institute of Technology, Bhopal, MP 462051 INDIA (phone: 91-9981232944; fax: 91-755-2670562; e-mail: vikastewari1@rediffmail.com).

K. R. Pardasani, is with the Maulana Azad National Institute of Technology, Bhopal, MP 462051 INDIA (phone: 91-9425358308; fax: 91-755-2670562; e-mail: kamalraj@rediffmail.com, kamalraj@hotmail.com).

$$[Ca^{2+}] + [B_j] \xrightleftharpoons[k^-]{k^+} [CaB_j] \quad (1)$$

where, [Bj] and [CaBj] are free and bound buffers respectively, and 'j' is an index over buffer species. Using Fick's law of diffusion and law of mass action we have the following partial differential equation [9],

$$\frac{\partial [Ca^{2+}]}{\partial t} = \beta (D_{Ca} + \gamma_m D_{CaB_m}) \nabla^2 [Ca^{2+}] - \frac{2\beta\gamma_m D_{CaB_m}}{K_m + [Ca^{2+}]} \nabla [Ca^{2+}] \cdot \nabla [Ca^{2+}]$$

where,

$$\beta = (1 + \gamma_s + \gamma_m)^{-1} \text{ and} \quad \gamma_m = \frac{K_m [B_m]_T}{(K_m + [Ca^{2+}])^2} \quad (2)$$

where,  $D_{Ca}$ ,  $D_{B_m}$  and  $D_{CaB_m}$  are the diffusion coefficients of free calcium, free buffer and calcium bound buffer respectively and  $K_m$  is disassociation rate constant. For stationary buffers  $D_{B_m}, D_{CaB_m} = 0$ .

The proposed mathematical model also contains the following parameters, to study the effect of rapid buffer and  $Na^+$  ions over  $Ca^{2+}$  diffusion,

#### A. Ion channels

The  $Ca^{2+}$  and  $Na^+$  channels have been modelled using the Goldman-Hodgkin-Katz(GHK) current equation [5],

$$I_s = P_s z_s^2 \frac{F^2 V_m}{RT} \frac{[S]_i - [S]_o \exp\left(-\frac{z_s F V_m}{RT}\right)}{\left(1 - \exp\left(-\frac{z_s F V_m}{RT}\right)\right)} \quad (3)$$

Where  $[S]_i, [S]_o$ , are the intracellular and extracellular ion concentration (Molar), respectively.  $P_s$  is the permeability (m/s) of S ion,  $z_s$  is valence of S ion. F is Faraday's constant (C/moles).  $V_m$  is membrane potential (Volts). R is Real gas constant (J/K moles) and T is Absolute temperature (Kelvin).

Equation (3) is converted into molar/second by using the following equation

$$\sigma_s = \frac{-I_s}{z_s F V_{cyt}} \quad (4)$$

The negative sign in equation (4) is taken because by convention inward current is taken to be negative. The GHK equation is derived from the *constant field approximation* which assumes that the electric field in the membrane is constant, and thus decoupled from the effects of charges moving through the membrane.

#### B. $Na^+/Ca^{2+}$ Exchange(NCX) Protein

The NCX protein is essential for excitation-contraction coupling in cardiac myocytes [4]. It helps in the extrusion of cytosolic calcium in neurons and hence regulates neurotransmitter release. In our model we have taken an exchange ratio of 4:1 with respect to sodium and calcium ions respectively [4]. The amount of energy required to extrude an ion against its concentration gradient is given by :

$$\Delta_s = z_s F V_m + RT \log \left( \frac{S_i}{S_o} \right) \quad (5)$$

So using  $\Delta Ca^{2+} = 4\Delta Na^+$  we have,

$$\sigma_{NCX} = Ca_o \left( \frac{Na_i}{Na_o} \right)^4 \exp \left( \frac{2FV_m}{RT} \right) \quad (6)$$

$$\bar{\sigma}_{NCX} = Na_o \left( \frac{Ca_i}{Ca_o} \right)^{1/4} \exp \left( -\frac{FV_m}{2RT} \right) \quad (7)$$

#### C. Sarcolemmal Calcium ATPase pump (SL CaATPase pump)

It is a P-type ATPase which is also known as Plasma Membrane Calcium ATPase pump (PMCA). Energy obtained from ATP is used to extrude calcium ions out of the cytosol. The kinetics of the pump follows Michaelis - Menten kinetics [7][2]. So the net efflux of calcium ions out of the cytosol is given by:

$$\sigma_{SLPump} = \frac{V_{SLPump}}{1 + \left( \frac{K_{SLPump}}{Ca_i} \right)^H} \quad (8)$$

where,  $V_{SLPump}$  is the maximum pump capacity,  $K_{SLPump}$  is half of the maximum pump capacity at steady state and H is the Hill's coefficient.

Combining equations (1-8) we get the proposed mathematical model as given below,

$$\frac{\partial [Ca^{2+}]}{\partial t} = \beta \left( \begin{array}{l} (D_{Ca} + \gamma_m D_{CaB_m}) \nabla^2 [Ca^{2+}] \\ - \frac{2\gamma_m D_{CaB_m}}{K_m + [Ca^{2+}]} \nabla [Ca^{2+}] \cdot \nabla [Ca^{2+}] \\ - \sigma_{NCX} - \sigma_{SLPump} \end{array} \right) \quad (9)$$

$$\frac{\partial [Na^+]}{\partial t} = \beta_{sod} (-\sigma_{Na} + \sigma_{NCX}) \quad (10)$$

Along with the initial-boundary conditions,

Initial condition:

$$[Ca^{2+}]_{t=0} = 0.1 \mu M \quad (11)$$

$$[Na^+]_{t=0} = 12 m M$$

Boundary conditions:

$$\lim_{r \rightarrow 0} \left( -2\pi r^2 \beta (D_{Ca} + \gamma_m D_{CaB_m}) \frac{d[Ca^{2+}]}{dr} \right) = \beta \sigma_{Ca} \quad (12)$$

$$\lim_{r \rightarrow \infty} [Ca^{2+}] = 0.1 \mu M \quad (13)$$

Our problem is to solve equation (9) and (10) coupled with equations (11 - 13). For our convenience we are writing 'u' in lieu of  $[Ca^{2+}]$  and 'v' in lieu of  $[Na^+]$ . Applying finite difference method (Forward Time Centered Space) on

equation (9) and (10), we get

$$\frac{u_i^{j+1}-u_i^j}{k} = \beta_i^j \left( \begin{aligned} & \left( (Def f)_i^j \frac{(u_{i+1}^j-2u_i^j+u_{i-1}^j)}{(h^2)} \right) \\ & + \frac{(u_{i+1}^j-u_{i-1}^j)}{h} \left( \frac{Def f_i^j}{r_i} - \frac{((\gamma_m^j D_m)(u_{i+1}^j-u_{i-1}^j))}{(2h(K_m+u_i^j))} \right) \\ & - u_{out} \left( \frac{v_i^j}{v_{out}} \right)^4 e^{2\varepsilon} - \frac{V_{SLPump}}{1+\left(\frac{K_{SLPump}}{u_i^j}\right)^{1.6}} \end{aligned} \right)$$

$$\frac{v_i^{j+1}-v_i^j}{k} = \beta_{sod}^j \left( v_{out} \left( \frac{u_i^j}{u_{out}} \right)^{(1/4)} e^{(-\varepsilon/2)} + \frac{((3*10^5) P_{Na} \varepsilon)}{(1-e^\varepsilon)} (v_i^j e^\varepsilon - v_{out}) \right) \quad (14)$$

where,  $\varepsilon = FV_m/RT$  is a dimensionless quantity, 'h' represents spatial step and 'k' represents time step, 'i' and 'j' represents the index of space and time respectively. Since, the above expression is not valid at the mouth of the channel; therefore the approximation at the mouth of the channel is given by

$$u_1^{j+1} = \beta_1^j \cdot k \cdot \left[ (Def f)_1^j \cdot \frac{(2u_2^j-2u_1^j)}{(h^2)} + \sigma_1^j - u_{out} \left( \frac{v_1^j}{v_{out}} \right)^4 e^{2\varepsilon} - \frac{V_{SLPump}}{1+\left(\frac{K_{SLPump}}{u_1^j}\right)^{1.6}} \right] + u_1^j$$

$$v_1^{j+1} = k \cdot \beta_{sod}^j \left[ v_{out} \left( \frac{u_1^j}{u_{out}} \right)^{(1/4)} e^{(-\varepsilon/2)} + \frac{((3*10^5) P_{Na} \varepsilon)}{(1-e^\varepsilon)} (v_1^j e^\varepsilon - v_{out}) \right] + v_1^j \quad (15)$$

Where,  $p = \frac{Def f k}{h^2}$ ,  $A = \frac{u_{out}}{(v_{out})^4} e^\varepsilon k$ ,  $Z = V_{SLPump} k$ ,  $Def f = D_{Ca} + \gamma_m D_m$

Approximation for rest of the nodes is given by,

$$u_i^{j+1} = k \cdot \beta_i^j \left[ \left( (Def f)_i^j \frac{(u_{i+1}^j-2u_i^j+u_{i-1}^j)}{(h^2)} \right) + \frac{(u_{i+1}^j-u_{i-1}^j)}{h} \left( \frac{Def f_i^j}{r_i} - \frac{((\gamma_m^j D_m)(u_{i+1}^j-u_{i-1}^j))}{(2h(K_m+u_i^j))} \right) - u_{out} \left( \frac{v_i^j}{v_{out}} \right)^4 e^{2\varepsilon} - \frac{V_{SLPump}}{1+\left(\frac{K_{SLPump}}{u_i^j}\right)^{1.6}} \right] + u_i^j \quad (16)$$

The numerical results are computed using a program developed in MATLAB on a Pentium IV Dual Core,1.00 GB RAM,1.73GHz processor.

### III. RESULTS AND DISCUSSION

In this section we have shown the results for calcium profile against different biophysical parameters. The biophysical parameters used in the proposed model are as stated in the table below unless stated along with figures. Figures [1-6] show variation for mobile buffers. Figures [1-3] show variation of  $[Ca^{2+}]$  with respect to space. Figures [4-6] show variation of  $[Ca^{2+}]$  with respect to time where the time limit is taken to be

TABLE I  
VALUES OF BIOPHYSICAL PARAMETERS USED

Symbol	Parameter	Value	Reference
F	Faraday's Constant	96487 Coulombs/Mole	Known fact
R	Gas Constant	8.314 Joule / Kelvin Mole	Known fact
T	Absolute Temperature	310 °K	In this paper
$P_{Ca}$	Calcium Permeability $[Ca^{2+}]$	$5.4 \times 10^{-4}$ metre $s^{-1}$	In this paper
$P_{Na}$	Sodium Permeability $[Na^+]$	$6.07 \times 10^{-10}$ metre $s^{-1}$	[11]
$z_{Ca}$	Calcium valence	2	Known fact
$z_{Na}$	Sodium valence	1	Known fact
$V_m$	Resting membrane potential	-0.07 Volts	[3]
$[Na^+]_i$	Cytosolic $[Na^+]$	12 mM	[8]
$[Na^+]_o$	Extracellular $[Na^+]$	145 mM	[8]
$[Ca^{2+}]_i$	Cytosolic $[Ca^{2+}]$	0.1 $\mu$ M	[8]
$[Ca^{2+}]_o$	Extracellular $[Ca^{2+}]$	1.8 mM	[8]
$D_{Ca}$	Diffusion coefficient	$250 \mu m^2 s^{-1}$	[11]
$D_m$	Mobile buffer diffusion coefficient	$32 \mu m^2 s^{-1}$	[10]
$K_m$	Mobile buffer disassociation rate	2 $\mu$ M	[10]
$K_s$	Stationary buffer disassociation rate	3 $\mu$ M	[10]
$K_{msod}$	Sodium mobile buffer disassociation rate	10 mM	[8]
$B_m$	Mobile buffer concentration	24 $\mu$ M	[8]
$B_s$	stationary buffer concentration	70 $\mu$ M	[8]
$B_{msod}$	Sodium mobile buffer concentration	5.35 mM	[8]
$V_{SLPump}$	Maximum pump capacity of PMCA	45 $\mu M s^{-1}$	[13]
$K_{SLPump}$	Half maximal pump capacity	0.1 $\mu$ M	[13]
H	Hill's coefficient	1.6	[8]

10 milliseconds. Figures [7,8] show variation of  $[Ca^{2+}]$  with time for stationary buffers.

#### Mobile buffers (Simulation time =240s)

Figure1 shows the variation of calcium concentration with buffer concentration and space. Mobile buffers influence both the spatial and temporal calcium profiles. Since in RBA the buffer binding kinetics is faster than calcium diffusion the variation of calcium with space is very rapid. To see the effects of buffer more clearly the log scale of space has been taken. The figure is in agreement with the biophysical facts. As the buffer concentration increases there are more number

of sites available for calcium binding and thus the calcium concentration decreases. The calcium concentration eventually achieves steady state as we move away from the source.

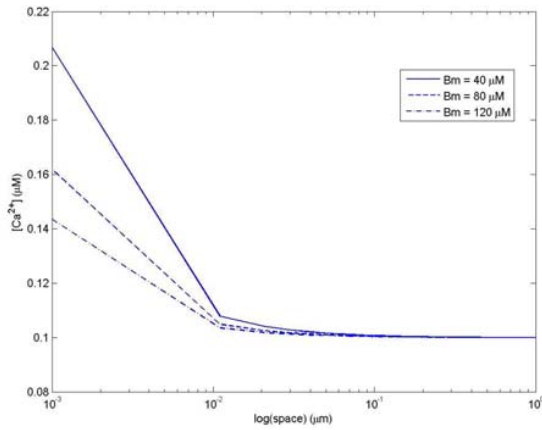


Fig 1. Variation of calcium with respect to space and mobile buffer concentration. Parameters: As stated in the Table I.

Steady state is achieved when the inflow of calcium ions via L-type calcium channels is balanced by an equal amount of calcium extrusion via NCX protein and Sarcolemmal pumps. It is observed that the calcium achieves steady state faster in rapid buffering approximation compared to excess buffering approximation.

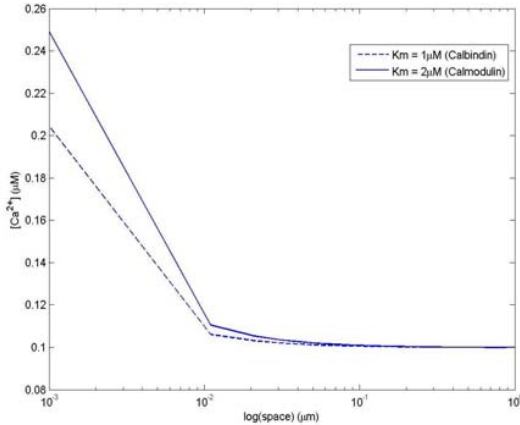


Fig. 2. Variation of calcium with space and Mobile buffer Disassociation constant. Parameters: As stated in the Table I.

The above figure shows variation of calcium concentration with buffer disassociation rate. We have considered two different endogenous mobile buffers, calbindin ( $K_m=1\mu M$ ) and calmodulin ( $K_m=2\mu M$ ). The disassociation rate is the ratio of disassociation to association rates. Hence as the disassociation rate increases, more number of calcium ions gets free and lesser number of calcium ions bind, hence the calcium concentration increases. The steady state value of  $0.1\mu M$  for calcium in the cytosol is rapidly achieved.

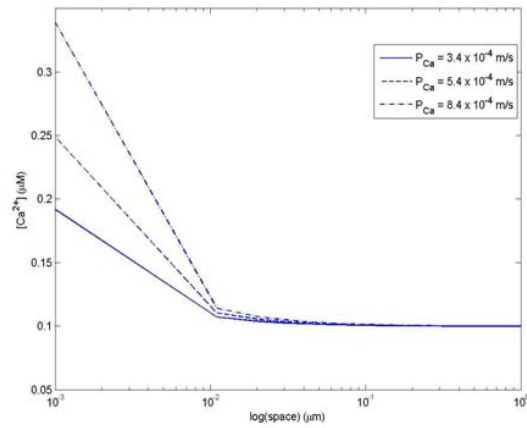


Fig. 3. Variation of calcium with space and calcium permeability. Parameters: As stated in the Table I.

In the above figure we have shown the spatial variation of calcium concentration with permeability of calcium. The permeability has a profound effect on the calcium concentration as is evident in the figure. As the permeability increases, more amount of calcium ions enter into the cytosol through the L-type calcium channel hence the calcium concentration increases. As the permeability is increased, the calcium ions inflow exceeds the outflow due to NCX protein and Sarcolemmal pump i.e.,

$$[Ca^{2+}]_{inflow} > \sigma_{NCX} + \sigma_{SLPump}$$

And hence there is a net inflow of calcium ions and thus the calcium concentration increases.

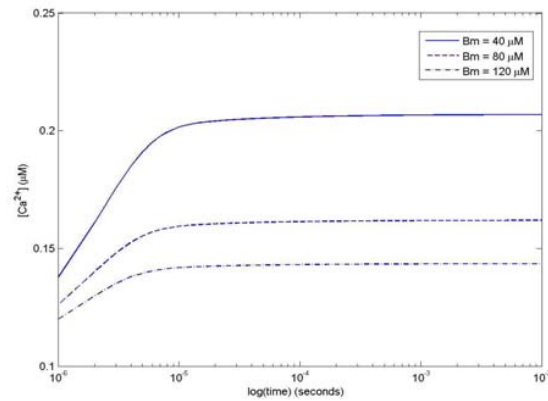


Fig. 4. Variation of calcium with time and Mobile buffer concentration Parameters: As stated in the Table I.

The above figure shows the temporal calcium profile. Log of time scale has been taken as the change was very rapid. The variations shown with respect to buffer concentration are in agreement with the biophysical facts. As the buffer concentration increases the calcium concentration decreases. The calcium concentration achieves steady state fast compared to EBA. For simulation of EBA we had taken minimum time of 100ms whereas in-case of RBA we have taken 10ms. The

steady state is achieved when the inflow of calcium ions from the L-type calcium channels is balanced by the outflow due to NCX protein and Sarcolemmal pump. The maximum value achieved by calcium is about  $0.2\mu\text{M}$  which is very low compared to the extracellular concentration of  $1.8\text{mM}$ . It is so because we have not incorporated the calcium concentration changes due to the Endoplasmic Reticulum in this model.

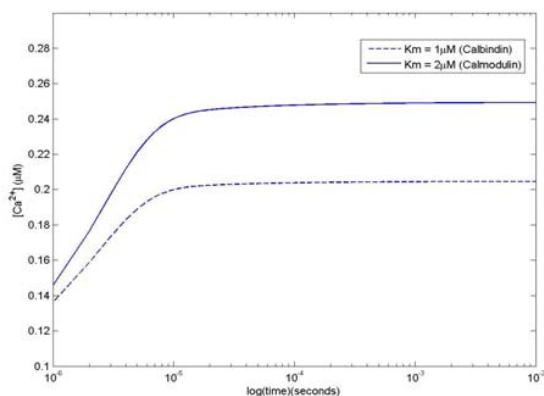


Fig. 5. Variation of calcium with time and Mobile buffer Disassociation rate Parameters: As stated in the Table I.

The above figure shows the variation of calcium concentration with disassociation rate. The two buffers considered here are calbindin ( $K_m=1\ \mu\text{M}$ ) and calmodulin ( $K_m=2\ \mu\text{M}$ ). As the disassociation rate increases more calcium ions become free and hence the calcium concentration increases. Using mobile endogenous buffers decreases the mobility of calcium ions as they get bound to the buffer but the range of calcium is increased [1]. The range is increased as the ions get carried a longer distance by the mobile buffers.

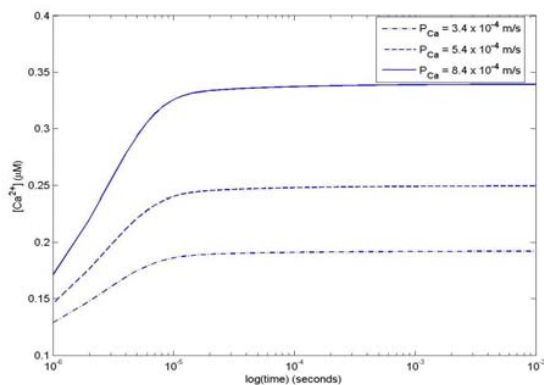


Fig. 6. Variation of calcium with time and calcium permeability Parameters: As stated in the Table I.

In the above figure we have shown the temporal variation of calcium concentration with permeability of calcium. The permeability has a profound effect on the calcium concentration as changing the permeability by a slight amount has a great effect on the calcium profile. The source amplitude ( $\sigma$ ) is directly proportional to the permeability of calcium ions. So as the permeability increases, more amount of calcium

ions enter into the cytosol through the L-type calcium channel hence the calcium concentration increases. This can be stated mathematically as follows,

$$[Ca^{2+}]_{inflow} > \sigma_{NCX} + \sigma_{SLPump}$$

Eventually, the inflow of calcium ions is balanced by the outflow and the calcium attains steady state.

**Stationary buffers** (only affect temporal variations)

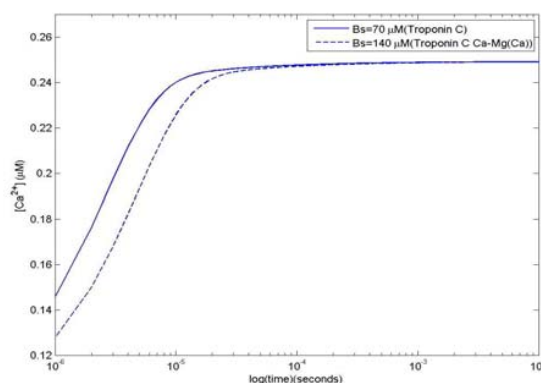


Fig. 7. Variation of calcium with time and Stationary buffer concentration Parameters: As in Table I.

Figure 7 shows the variation of calcium with stationary buffer concentration. The RBA is more realistic compared to EBA as we consider both the mobile and stationary buffers. Stationary buffers only affect the temporal profile and not the spatial profile as the buffers are immobile. We have considered two very common buffers for this study, these are Troponin C and Troponin C Ca-Mg (Ca). As the buffer concentration increases the calcium concentration decreases as there is an increase in calcium binding sites due to increase in buffer concentration.

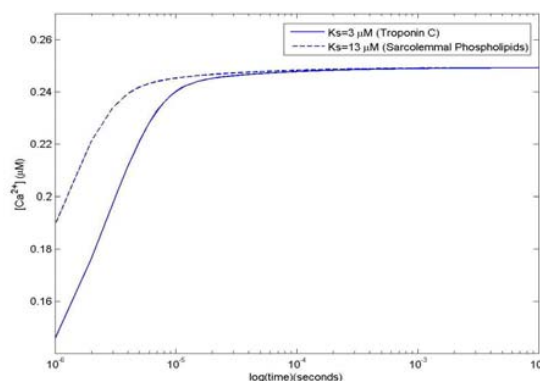


Fig. 8. Variation of calcium with time and Stationary buffer Disassociation rate Parameters: As stated in the Table I.

The above figure shows the variation of calcium concentration with disassociation rate. The two buffers considered in the figure are Troponin C ( $K_s=3\ \mu\text{M}$ ) and Sarcolemmal phospholipids ( $K_s=13\ \mu\text{M}$ ). As the disassociation rate increases from  $3\mu\text{M}$  to  $13\mu\text{M}$ , more calcium ions become free and hence

the calcium concentration increases. The calcium achieves a steady state after some time.

Some of the results shown in this paper are in agreement with the results obtained by previous researchers (Neher, Smith, Wagner and Keizer). The new results shown are also in agreement with the physiological facts. The results obtained in this paper may be useful to biomedical scientists for development of new protocols for treatment and diagnosis of neurological diseases.

#### APPENDIX

Using Laplacian operator '∇' in spherical symmetry, we have

$$\nabla^2 = \frac{\partial^2}{\partial r^2} + \frac{2}{r} \frac{\partial}{\partial r} \quad (17)$$

Further, we have used Forward Time Centered Space (FTCS) technique to solve eqn. (9) i.e.

$$\begin{aligned} \frac{\partial u}{\partial t} &\approx \frac{u_{i+1}^j - u_{i-1}^j}{k} \\ \frac{du}{dr} &\approx \frac{u_{i+1}^j - u_{i-1}^j}{2h} \\ \frac{d^2u}{dr^2} &\approx \frac{u_{i+1}^j - 2u_i^j + u_{i-1}^j}{h^2} \end{aligned} \quad (18)$$

Using equation(18) in equation(9) and solving we get equation(14) i.e.

$$\frac{u_{i+1}^j - u_i^j}{k} = \beta_i^j \left( \begin{aligned} &\left( (D_{eff})_i^j \frac{(u_{i+1}^j - 2u_i^j + u_{i-1}^j)}{h^2} \right) \\ &+ \frac{(u_{i+1}^j - u_{i-1}^j)}{h} \\ &\left( \frac{D_{eff}^j}{r_i} - \frac{((\gamma_m^j D_m)(u_{i+1}^j - u_{i-1}^j))}{(2h(K_m + u_i^j))} \right) \\ &- u_{out} \left( \frac{v_i^j}{v_{out}} \right)^4 e^{2\varepsilon} - \frac{V_{SLPump}}{1 + \left( \frac{K_{SLPump}}{u_i^j} \right)^{1.6}} \end{aligned} \right)$$

But this approximation does not hold for  $i = 1$ , as it gives rise to an imaginary node  $u_0^j$ . To eliminate this problem, we have used centered difference over equation (12) to yield,

$$u_0^j \approx u_2^j - \frac{2PCa\varepsilon h}{(1 - e^{2\varepsilon})\pi r_0^2 D_{eff}} (u_0^j e^{2\varepsilon} - u_{out})$$

Here, the scale used for distance was [0.0001, 1.0001]  $\mu\text{m}$ . Thus for  $i = 1$ , we have equation (15)i.e.

$$\begin{aligned} u_1^{j+1} &= \beta_1^j \cdot k \cdot \left[ (D_{eff})_1^j \cdot \frac{(2u_2^j - 2u_1^j)}{h^2} + \sigma_1^j - u_{out} \left( \frac{v_1^j}{v_{out}} \right)^4 e^{2\varepsilon} \right. \\ &\quad \left. - \frac{V_{SLPump}}{1 + \left( \frac{K_{SLPump}}{u_1^j} \right)^{1.6}} \right] + u_1^j \end{aligned}$$

#### ACKNOWLEDGMENT

The authors are highly grateful to Department of Biotechnology, New Delhi, India for providing support in the form of Bioinformatics Infrastructure Facility for carrying out this work.

#### REFERENCES

- [1] N.L. Allbritton, T. Meyer, and L. Stryer, *Range of messenger action of calcium ion and inositol 1,4,5-trisphosphate*, Science, 258, 1812-1815, 1992.
- [2] K.T. Blackwell, *Modeling Calcium Concentration and Biochemical Reactions*, Brains Minds and Media 1, 1-27, 2005.
- [3] G.L. Fain, *Molecular and cellular physiology of neurons*, Harvard University Press, 1999.
- [4] Y. Fujioka, K. Hiroe, S. Matsuoka, *Regulation kinetics of  $Na^+$ - $Ca^{2+}$  exchange current in guinea-pig ventricular myocytes*, J. Physiol. 529, 611-623, 2000.
- [5] J. Keener and J. Sneyd, *Mathematical Physiology*, Vol. 8, Springer, pp. 53 - 56, 1998.
- [6] E. Neher, *Concentration profiles of intracellular  $Ca^{2+}$  in the presence of diffusible chelators*, Exp. Brain Res. Ser., vol. 14, 80-96, 1986.
- [7] D.L. Nelson, M.M. Cox, *Lehninger Principles of Biochemistry*, 2005.
- [8] T.R. Shannon, F. Wang, F. Puglisi, C. Weber, D.M. Bers, *A Mathematical Treatment of Integrated  $Ca^{2+}$  Dynamics Within the Ventricular Myocyte*, Biophys.J. 87, 3351 - 3371, 2004.
- [9] G.D. Smith, *Analytical Steady-State Solution to the rapid buffering approximation near an open  $Ca^{2+}$  channel*, Biophys. J., vol. 71, 3064-3072, 1996.
- [10] G.D. Smith, J. Wagner, and J. Keizer *Validity of the rapid buffering approximation near a point source of calcium ions*, Biophys. J., vol. 70, 2527-2539, 1996.
- [11] S. Tewari and K.R. Pardasani, *Finite Difference Model to Study the Effects of  $Na^+$  Influx on Cytosolic  $Ca^{2+}$  Diffusion*, International Journal of Biological and Medical Sciences 1; 4,205-210,2008.
- [12] J. Wagner, J. Keizer, *Effects of Rapid Buffers on  $Ca^{2+}$  Diffusion and  $Ca^{2+}$  Oscillations*, Biophys. J., vol. 67, 447-456, 1994.
- [13] M.S. Jafri, J. Keizer, *On the Roles of  $Ca^{2+}$  Diffusion,  $Ca^{2+}$  Buffers, and the Endoplasmic Reticulum in  $IP_3$  - Induced  $Ca^{2+}$  Waves*, Biophys. J., vol. 69, 2139-2153, 1995.